

A Model of a Turbulent Boundary Layer With a Non-Zero Pressure Gradient

G. I. BARENBLATT,* A. J. CHORIN*
AND V. M. PROSTOKISHIN†

*Department of Mathematics and
Lawrence Berkeley National Laboratory,
University of California, Berkeley, California 94720–3840;

†P. P. Shirshov Institute of Oceanology,
Russian Academy of Sciences,
36 Nakhimov Prospect, Moscow 117218 Russia

Key Words: turbulent boundary layer, pressure gradient, self-similarity, scaling laws.

Contributed by G. I. Barenblatt

Abstract. According to a model of the turbulent boundary layer proposed by the authors, in the absence of external turbulence the intermediate region between the viscous sublayer and the external flow consists of two sharply separated self-similar structures. The velocity distribution in these structures is described by two different scaling laws. The mean velocity u in the region adjacent to the viscous sublayer is described by the previously obtained Reynolds-number-dependent scaling law $\phi = u/u_* = A\eta^\alpha$, $A = \frac{1}{\sqrt{3}} \ln Re_\Lambda + \frac{5}{2}$, $\alpha = \frac{3}{2 \ln Re_\Lambda}$, $\eta = u_* y / \nu$. (Here u_* is the dynamic or friction velocity, y is the distance from the wall, ν the kinematic viscosity of the fluid, and the Reynolds number Re_Λ is well defined by the data) In the region adjacent to the external flow the scaling law is different: $\phi = B\eta^\beta$. The power β for zero-pressure-gradient boundary layers was found by processing various experimental data and is close (with some scatter) to 0.2.

We show here that for non-zero-pressure-gradient boundary layers, the power β is larger than 0.2 in the case of adverse pressure gradient and less than 0.2 for favourable pressure gradient. Similarity analysis suggests that both the coefficient B and the power β depend on Re_Λ and on a new dimensionless parameter P proportional to the pressure gradient. Recent experimental data of Perry, Marušić and Jones (1)-(4) were analyzed and the results are in agreement with the model we propose.

1 Introduction

The model of the turbulent boundary layer at large Reynolds number proposed by Clauser (5) and Coles (6) is widely accepted and used. This model is based on the assumption that the transition from the wall region described by the Karman-Prandtl (7)-(8) universal logarithmic law to the external flow is smooth. On the basis of our analysis of experimental data published over the last 30 years we arrived at a different model (see (9)-(11)). According to our model, if the intensity of turbulence in the external flow is low, then the intermediate region between the viscous sublayer and the external flow consists of two self-similar structures separated by a sharp boundary. In particular, when the bilogarithmic coordinates $\lg \phi$, $\lg \eta$ are used, where $\phi = u/u_*$, $\eta = u_*y/\nu$, the mean velocity profile in the intermediate region has a characteristic form of a broken line ('chevron') (Figure 1). In part I of the intermediate region the scaling law for the mean velocity distribution takes the form:

$$\frac{u}{u_*} = A \left(\frac{u_*y}{\nu} \right)^\alpha . \quad [1]$$

In part II one finds a different scaling law:

$$\frac{u}{u_*} = B \left(\frac{u_*y}{\nu} \right)^\beta . \quad [2]$$

The constants A, α, B, β can be determined with sufficient accuracy by processing the experimental data. According to our model the expressions for A and α are identical to those in smooth pipes once the Reynolds number is defined correctly:

$$A = \frac{1}{\sqrt{3}} \ln Re_\Lambda + \frac{5}{2}, \quad \alpha = \frac{3}{2 \ln Re_\Lambda} . \quad [3]$$

Here Re_Λ is an effective Reynolds number for turbulent boundary layer, different from the usual Reynolds number Re_θ based on momentum thickness which is arbitrarily though widely used in turbulent boundary layer studies. The test of the validity of our model is the closeness of two values of $\ln Re_\Lambda$, $\ln Re_1$ and $\ln Re_2$, obtained by solving separately the two equations [3] with parameters A and α obtained from experimental data. Differences of less than 2–3% were obtained in all cases (see (10),(11) for previous data processing), and therefore we proposed to take $\ln Re_\Lambda$ as half the sum $\frac{1}{2}(\ln Re_1 + \ln Re_2)$.

In region II the power β in the scaling law [2] for the zero-pressure-gradient boundary layer was found to be close to 0.2 (with some scatter). In cases of non-zero-pressure-gradient boundary layers the values of β were found to be significantly different from 0.2. In the present Note we perform the similarity analysis for non-zero-pressure-gradient turbulent

boundary layer. We find that both the coefficient B and the power β depend on Re_Λ and on a new similarity parameter $P = \nu \partial_x p / \rho u_*^3$. We compare the results of this analysis with high quality experimental data by Marušić and Perry(1), Marušić (2), Jones, Marušić and Perry (3), Jones (4), and come to the instructive conclusions.

2 The model and the similarity analysis

According to our model the turbulent boundary layer at large Reynolds numbers consists of two separate layers I and II. The structure of the vorticity fields in the two layers is different although both are self-similar. In layer I the vortical structure is the one common to all developed wall-bounded shear flows and the mean flow velocity is described by relations [1] and [3]. In these relations $Re_\Lambda = U\Lambda/\nu$, where Λ is a characteristic length (12) close to 1.6 of the height of layer I.

The influence of viscosity is transmitted to the main body of the flow via streaks separating from the viscous sublayer.¹ The remaining part of the intermediate region of the boundary layer is occupied by layer II where the relation [2] holds. It is well known (see in particular instructive photographs in Van Dyke's *Album of Fluid Motions* (13)) that the upper boundary of the boundary layer is covered with statistical regularity by large scale 'humps' and that the upper layer is influenced by the external flow via the form drag of these humps as well as by the shear stress. We have shown in earlier work that the mean velocity profile is affected by the intermittency of the turbulence, and as the humps affect intermittency it is natural to see two different scaling regions. On the basis of these considerations we have to determine a set of parameters that determine the coefficient B and the power β in [2]. One of these parameters must be the effective Reynolds number Re_Λ which determines the flow structure in the layer I and is affected in its turn by the viscous sublayer and by layer II. The following parameters should also influence the flow in the upper layer: the pressure gradient $\partial_x p$ (x is the longitudinal coordinate reckoned along the plate; its origin is immaterial), the dynamic (friction) velocity u_* , and the fluid's kinematic viscosity ν and density ρ . The dimensions of governing parameters are as follows

$$[\partial_x p] = \frac{M}{L^2 T^2}, \quad [u_*] = \frac{L}{T}, \quad [\nu] = \frac{L^2}{T}, \quad [\rho] = \frac{M}{L^3}. \quad [4]$$

¹We note that this mechanism for the molecular viscosity affecting the main body of the flow was proposed by L. Prandtl in his discussion of Th. von Kármán's lecture (8). It is rather astonishing that this idea was never repeated in Prandtl's subsequent publications.

The first three have independent dimensions so that only one dimensionless governing parameter can be formed:

$$P = \frac{\nu \partial_x p}{\rho u_*^3} \quad [5]$$

Thus the parameters B and β should depend on two the parameters Re_Λ and P :

$$B = B(Re_\Lambda, P), \quad \beta = \beta(Re_\Lambda, P). \quad [6]$$

3 Comparison with experimental data

The data for non-zero-pressure-gradient flows are substantially less numerous than data for zero-pressure-gradient flows, and do not allow us yet to construct surfaces $B(Re_\Lambda, P)$, $\beta(Re_\Lambda, P)$. However the high quality data obtained by Marušić and Perry [(1), recently brought to completion via the internet] and Jones, Marušić and Perry [(2), also completed on the internet] allowed us to come to some instructive conclusions. The experiments of Marušić and Perry (1) were performed for two external flow velocities U : 10 m/s and 30 m/s. The experiments of Jones, Marušić and Perry (3) were performed for three external flow velocities U : 5 m/s, 7.5 m/s, and 10 m/s. The results of the processing of the experimental data are presented in Table 1. Here \mathbf{x} and Re_θ are given by the authors of the experiments, and $\Delta = 2|\ln Re_1 - \ln Re_2|/(\ln Re_1 + \ln Re_2)$.

Table 1

\mathbf{x}, \mathbf{m}	Re_θ	α	A	β	B	$\ln Re_1$	$\ln Re_2$	$\ln Re_\Lambda$	Δ
I. Marušić data									
$U = 10 \text{ m/s}$									
1.20	2,206	0.143	8.53	0.203	6.18	10.44	10.51	10.48	0.7
1.80	3,153	0.150	8.30	0.227	5.45	10.05	10.03	10.04	0.2
2.24	4,155	0.156	8.15	0.269	4.34	9.79	9.88	9.84	0.9
2.64	5,395	0.171	7.54	0.345	2.87	8.73	8.77	8.75	0.5
2.88	6,358	0.167	7.63	0.408	2.00	8.89	8.98	8.93	1.1
3.08	7,257	0.169	7.57	0.450	1.64	8.78	8.88	8.83	1.2
$U = 30 \text{ m/s}$									
1.20	6,430	0.140	8.45	0.190	6.08	10.30	10.72	10.51	3.9
1.80	8,588	0.145	8.41	0.207	5.63	10.24	10.32	10.28	0.8
1.24	10,997	0.145	8.44	0.247	4.31	10.29	10.32	10.31	0.4
2.64	14,208	0.147	8.39	0.306	2.91	10.20	10.20	10.20	0.1
2.88	16,584	0.148	8.38	0.346	2.23	10.19	10.17	10.18	0.2
3.08	19,133	0.145	8.45	0.388	1.71	10.31	10.35	10.33	0.4

M.B. Jones data	x, m	Re_θ	α	A	β	B	$\ln Re_1$	$\ln Re_2$	$\ln Re_\Lambda$	Δ
	$U = 10 \text{ m/s}$									
	0.18	855	0.144	8.39	0.20	6.36	10.21	10.45	10.33	2.4
	0.40	1,122	0.144	8.37	0.176	7.11	10.17	10.40	10.29	2.2
	0.60	1,314	0.146	8.28	0.168	7.41	10.01	10.25	10.13	2.4
	0.80	1,466	0.148	8.19	0.166	7.47	9.86	10.11	9.98	2.5
	1.00	1,616	0.144	8.38	0.160	7.68	10.19	10.44	10.31	2.5
	1.20	1,745	0.145	8.35	0.156	7.84	10.13	10.38	10.25	2.4
	1.40	1,888	0.142	8.44	0.153	7.99	10.29	10.55	10.42	2.5
	1.60	2,039	0.142	8.45	0.150	8.10	10.28	10.53	10.41	2.4
	1.80	2,150	0.143	8.41	0.148	8.18	10.23	10.50	10.36	2.6
	2.00	2,299	0.141	8.49	0.144	8.35	10.37	10.62	10.50	2.4
	2.20	2,411	0.144	8.37	—	—	10.17	10.43	10.30	2.5
	2.40	2,489	0.139	8.57	—	—	10.52	10.78	10.65	2.4
	2.60	2,574	0.145	8.32	—	—	10.08	10.36	10.22	2.7
	2.80	2,683	0.142	8.47	—	—	10.34	10.60	10.47	2.5
	2.92	2,728	0.145	8.31	—	—	10.06	10.33	10.19	2.7
	3.04	2,819	0.149	8.15	—	—	9.79	10.06	9.92	2.8
	3.16	2,832	0.147	8.24	—	—	9.94	10.20	10.07	2.6
	3.28	2,946	0.149	8.14	—	—	9.77	10.05	9.91	2.8
	3.40	2,987	0.142	8.46	—	—	10.32	10.60	10.46	2.7
	3.48	3,026	0.145	8.33	—	—	10.11	10.38	10.24	2.7
	3.54	3,032	0.146	8.29	—	—	10.03	10.30	10.16	2.7
	3.58	3,100	0.146	8.27	—	—	9.99	10.28	10.13	2.9
	3.62	3,029	0.147	8.20	—	—	9.88	10.20	10.04	3.2

For our subsequent analysis we will use the series corresponding to $U = 30 \text{ m/s}$ of (2) and $U = 10 \text{ m/s}$ of (4) for the following reasons: in spite of a considerable variation in the usual parameter Re_θ , the effective Reynolds number Re_Λ obtained by the the procedure we introduced remains nearly constant and close, for $U = 30 \text{ m/s}$ (2), to a constant $\ln Re_\Lambda = 10.3$, and for $U = 10 \text{ m/s}$ (4) to a constant $\ln Re_\Lambda = 10.2$. The mean velocity distribution in bilogarithmic coordinates for both series is presented in Figure 2. Thus, we are able to obtain, with some approximation, cross-sections of the surfaces $B(Re_\Lambda, P)$, $\beta(Re_\Lambda, P)$. The results corresponding to $\ln Re_\Lambda = 10.3$ (adverse pressure gradient) are presented in Figures 3(a) and 3(b); results corresponding to $\ln Re_\Lambda = 10.2$ (favourable pressure gradient) are presented in Figures 3(c) and 3(d). Note that for large values of the favourable pressure gradient we were unable to reveal the second self-similar region. The situation is reminiscent

of the disappearance of the second self-similar region in flows with an elevated level of free-stream turbulence. We found such a situation previously (10) when we processed the results of the remarkable experimental work of P.E. Hancock and P. Bradshaw (14).

In the papers (1)-(4) the results concerning pressure were presented through a coefficient

$$C_p = \frac{p - p_\infty}{\frac{1}{2}\rho U^2}$$

where p_∞ is a constant reference pressure. Therefore we calculated the parameter P using the relation $\partial_x p = \frac{1}{2}\rho U^2 \partial_x C_p$ where the density ρ cancelled out; the values of all the other parameters are available in (2),(4). The values of the parameter P for $U = 30$ m/s (2) and for $U = 10$ m/s (4) are presented in Table 2.

Table 2

I.Marusic							
Re_θ	6,430	8,588	10,997	14,208	16,584	19,133	
$P * 10^3$	0	1.75	2.86	4.2	5.79	7.04	
$\ln Re_\Lambda$	10.5	10.3	10.3	10.2	10.2	10.3	
M.B.Jones							
Re_θ	855	1,122	1,314	1,466	1,616	1,745	
$-P * 10^3$	1.8	2.36	2.69	2.78	2.76	2.8	
$\ln Re_\Lambda$	10.3	10.3	10.1	10.0	10.3	10.2	

Eliminating the parameter P from relations [6], we obtain:

$$B = B(Re_\Lambda, \beta) . \quad [7]$$

This relation is presented in Figure 4 in the form of a dependence of B on $\frac{1}{\beta}$. We see that this dependence is close to linear:

$$B = \frac{1.75}{\beta} - 2.80 \quad [8]$$

for the data by Marušić (2) (*adverse* pressure gradient) and

$$B = \frac{1}{\beta} + 1.43 \quad [9]$$

for the data by Jones (4) (*favourable* pressure gradient)

For layer I there is also a linear relation between the coefficients A and $\frac{1}{\alpha}$, but contrary to $B = B(\frac{1}{\beta})$ this relation is universal. The coefficients in the relation $B = B(\frac{1}{\beta})$ should in principle depend on Re_Λ .

4 Conclusion

A new similarity parameter is obtained for the flow in the upper self-similar region of a developed non-zero-pressure-gradient turbulent boundary layer. Comparison with experimental data for nearly constant effective Reynolds numbers revealed simple (close to linear) Reynolds number-dependent relations between the parameters of the scaling law for the mean velocity distributions in the upper self-similar layer.

The investigation performed in the present Note and the papers (9)-(12) demonstrated that the Reynolds number-dependent scaling law for the velocity distribution across the shear flow obtained initially for flows in pipes is valid (with the same values of the constants) for the developed turbulent boundary layer flows. This allows us to expect that this scaling law reflects a universal property of all developed shear flows. The Reynolds number entering the law cannot be selected arbitrarily, for example, as Re_θ : it is uniquely determined by the flow itself. The simple procedure for the determination of the appropriate Reynolds number, which we proposed earlier, has been further validated in the present Note.

We expect that the same approach will work for more complicated flows: mixing layers, jets and wall jets. However, the delicate task of investigating such flows requires high quality experimental data which are still lacking.

The concepts of incomplete similarity and vanishing viscosity asymptotics which we used for shear flows lead to plausible results for the local structure of developed turbulent flows. Here, however, high quality experimental data are very rare, specially for the higher order structure functions, where we have conjectured that divergences may occur.

Acknowledgement. The authors express their gratitude to Professor Ivan Marušić for clarification of experimental results. The work was supported by the Applied Mathematics subprogram of the U.S. Department of Energy under contract DE-AC03-76-SF00098.

References

1. Marušić, Ivan, and Perry, A.E. (1995). *J. Fluid Mech.* **298**, 389–407.
2. Marušić, I. (1991). The structure of zero and adverse-pressure gradient turbulent boundary layers. PhD thesis, University of Melbourne, Australia, (<http://www.mame.mu.oz.au/~ivan/>).
3. Jones, M.B., Marušić, Ivan, and Perry, A.E. (2001). *J. Fluid Mech.* **428**, 1–27.

4. Jones, M.B. (1998). Evolution and structure of sink-flow turbulent boundary layers. PhD thesis, University of Melbourne, Australia, (<http://www.mame.mu.oz.au/~mbjones/>).
5. Clauser, D.E. (1954). *J. Aero. Sci.* **21**, 91–108.
6. Coles, D.E. (1956). *J. Fluid Mech.* **1**, 1–51.
7. Prandtl, L. (1932). *Ergebn. Aerodyn. Versuchanstalt Gottingen* **4**, 18–29.
8. von Karman, Th. (1930). In: C.W.Oseen and W.Weibull (eds.), *Proc. 3rd Int. Cong. Appl. Mech.* AB Sveriges Litografiska Tryckerier, Stockholm. Vol. I, 85–93.
9. Barenblatt, G.I., Chorin, A.J., Hald, O.H., and Prostokishin, V.M. (1997). *Proc. Natl. Acad. Sci. USA* **94**, 7817–7819.
10. Barenblatt, G.I., Chorin, A.J., and Prostokishin, V.M. (2000). *J. Fluid Mech.* **410**, 263–283.
11. Barenblatt, G.I., Chorin, A.J., and Prostokishin, V.M. (2000). Ctr for Pure and Applied Mathematics, University of California, Berkeley, California, report CPAM–777.
12. Barenblatt, G.I., Chorin, A.J., and Prostokishin, V.M. (2000). *Proc. Natl. Acad. Sci. USA* **97**, 3799–3802.
13. Van Dyke, M. (1980). *An Album of Fluid Motion*. The Parabolic Press, Stanford, California.
14. Hancock, P.E., and Bradshaw, P. (1989). *J. Fluid Mech.* **205**, 45–76.

Figure Captions

Figure 1. Schematic representation of the mean velocity profile in developed turbulent boundary layer in bilogarithmic coordinates $\lg \frac{u}{u_*}$, $\lg \frac{u_* y}{\nu}$.

Figure 2. (a) The mean velocity profiles in bilogarithmic coordinates in the series of experiments of Marušić for $U = 30$ m/s; *adverse* pressure gradient .

- | | |
|--------------------------|---------------------------|
| (1) $Re_\theta = 19,133$ | (2) $Re_\theta = 16,584,$ |
| (3) $Re_\theta = 14,208$ | (4) $Re_\theta = 10,997,$ |
| (5) $Re_\theta = 8,588$ | (6) $Re_\theta = 6,430.$ |

The ‘chevron’ structure of the profiles is clearly seen and regions I and II are clearly distinguishable.

(b) The mean velocity profiles in bilogarithmic coordinates in the series of experiments of Jones for $U = 10$ m/s; *favourable* pressure gradient .

- | | |
|-------------------------|--------------------------|
| (1) $Re_\theta = 855$ | (2) $Re_\theta = 1,122,$ |
| (3) $Re_\theta = 1,314$ | (4) $Re_\theta = 1,616,$ |
| (5) $Re_\theta = 2,728$ | (6) $Re_\theta = 3,032.$ |

The ‘chevron’ structure of the profiles is clearly seen for the curves (1)–(4), where $\beta > \alpha$.

Figure 3. (a) Cross-section of the surface $\beta(Re_\Lambda, P)$, for $Re_\Lambda \cong 10.3$; (2).

(b) Cross-section of the surface $B(Re_\Lambda, P)$, for $Re_\Lambda \cong 10.3$; (2).

(c) Cross-section of the surface $\beta(Re_\Lambda, P)$, for $Re_\Lambda \cong 10.2$; (4).

(d) Cross-section of the surface $B(Re_\Lambda, P)$, for $Re_\Lambda \cong 10.2$; (4).

Figure 4. (a) The dependence $B(\frac{1}{\beta})$ for $Re_\Lambda \cong 10.3$;
the straight line corresponds to $1.75/\beta - 2.8$.

(b) The dependence $B(\frac{1}{\beta})$ for $Re_\Lambda \cong 10.2$;
the straight line corresponds to $1/\beta + 1.43$.

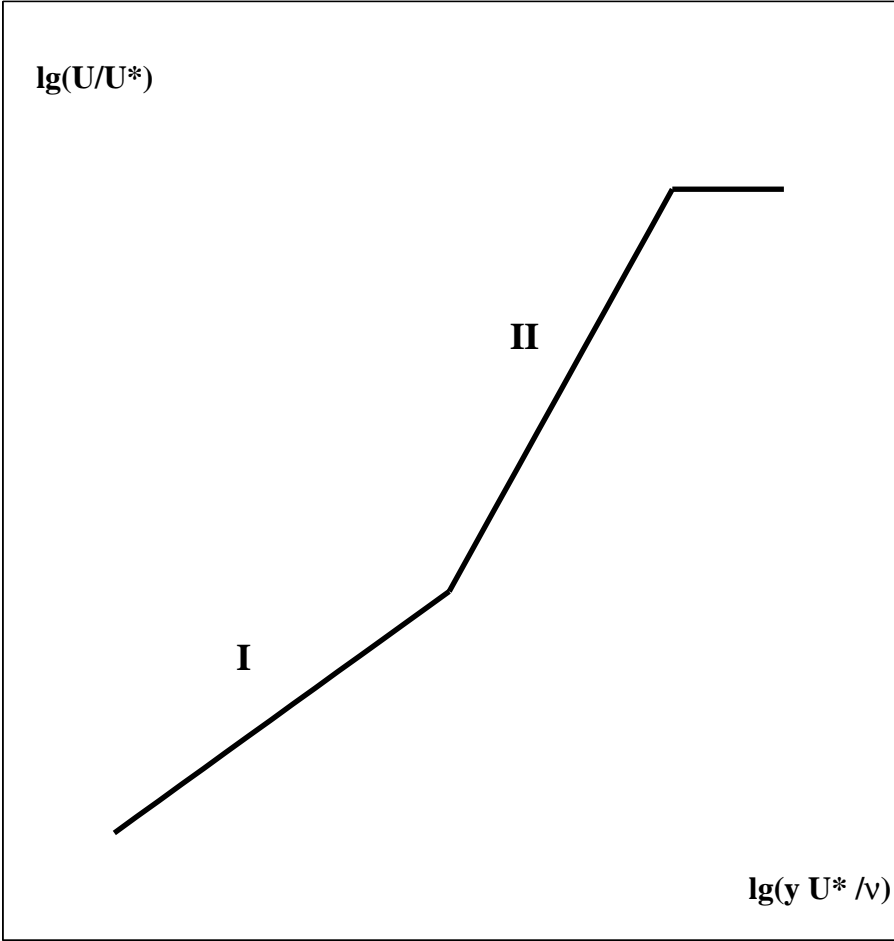


Figure 1

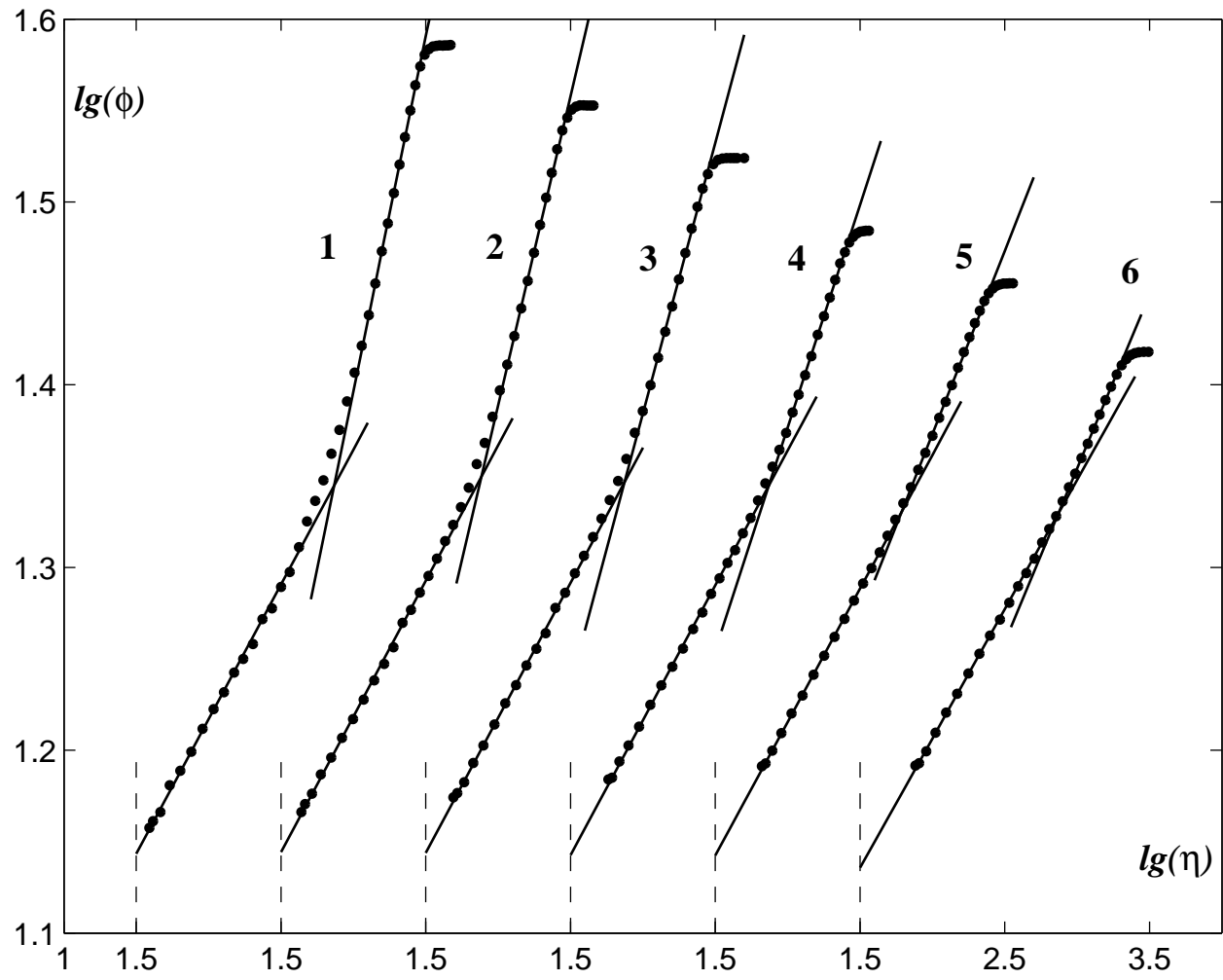


Figure 2 a

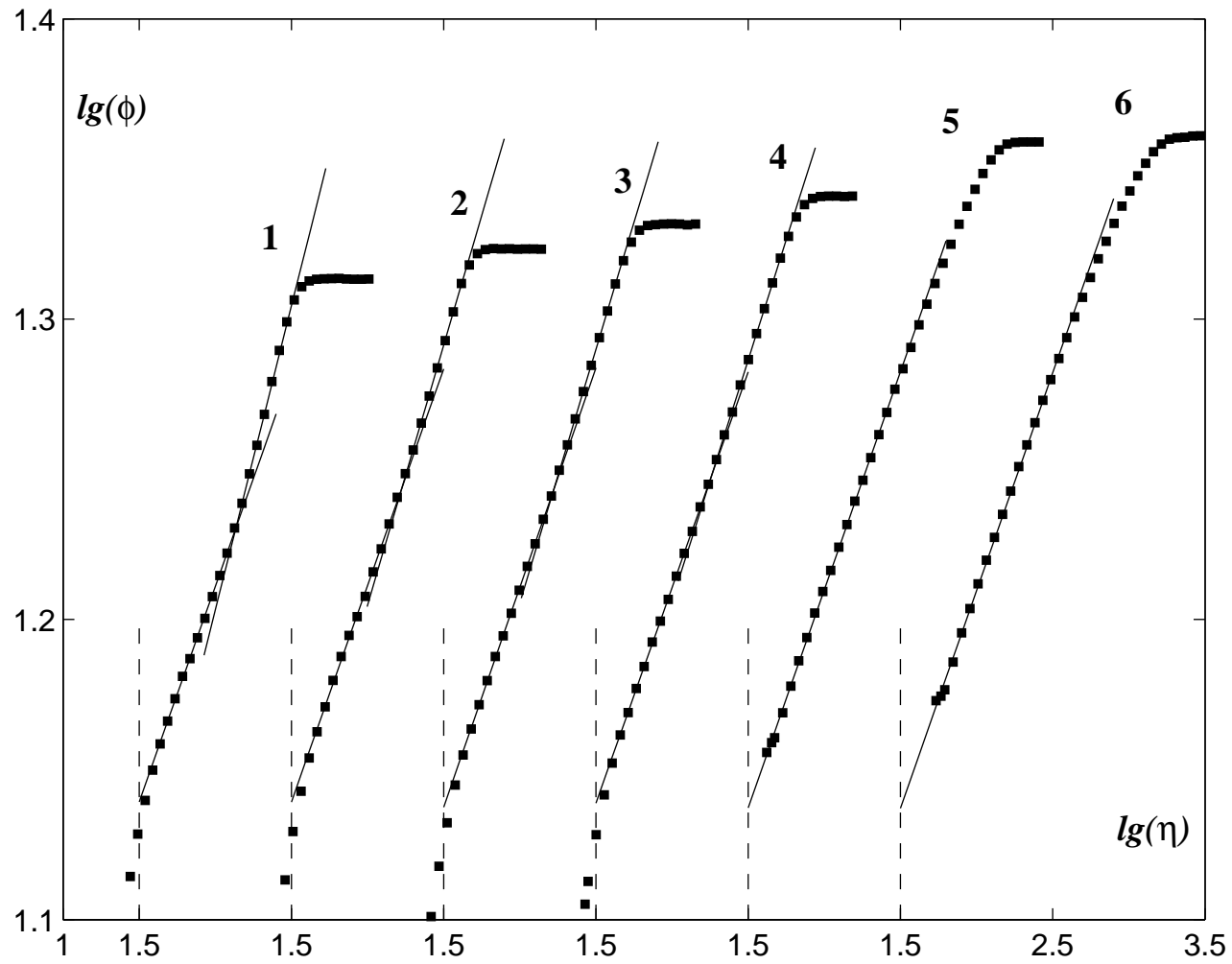


Figure 2 b

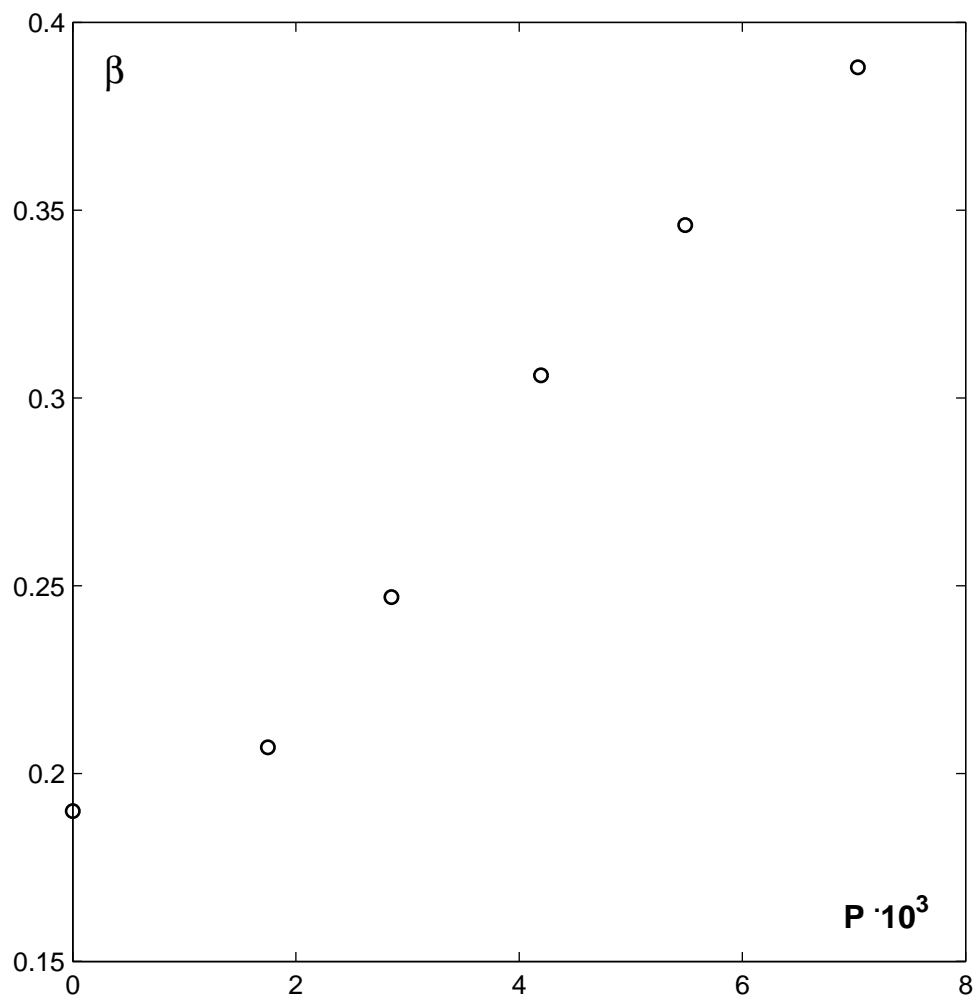


Figure 3 a

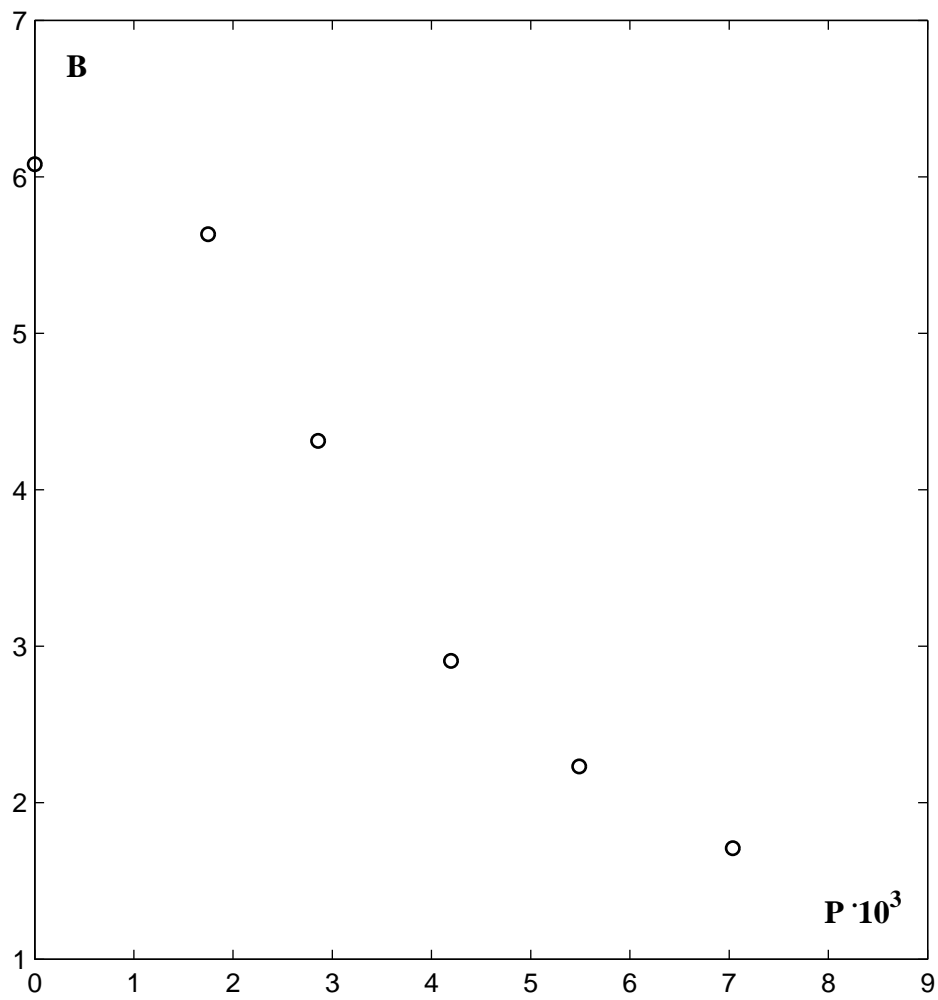


Figure 3 b

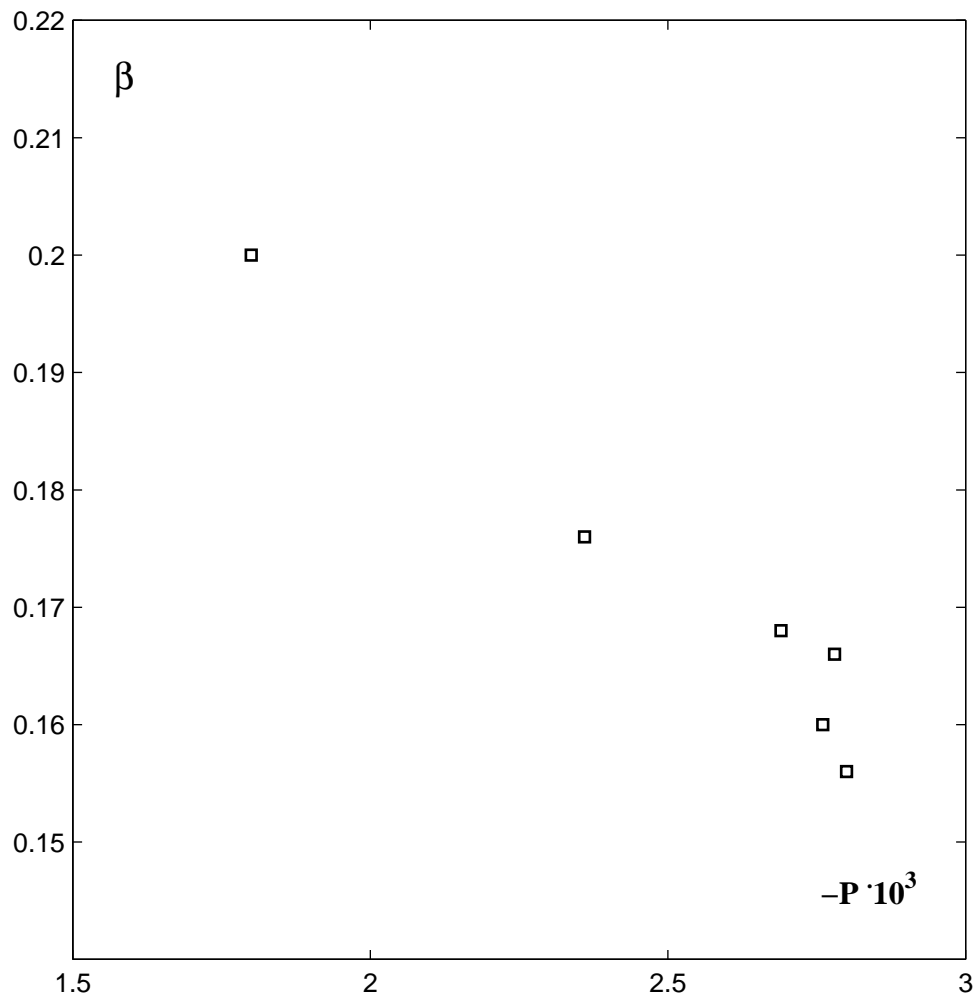


Figure 3 c

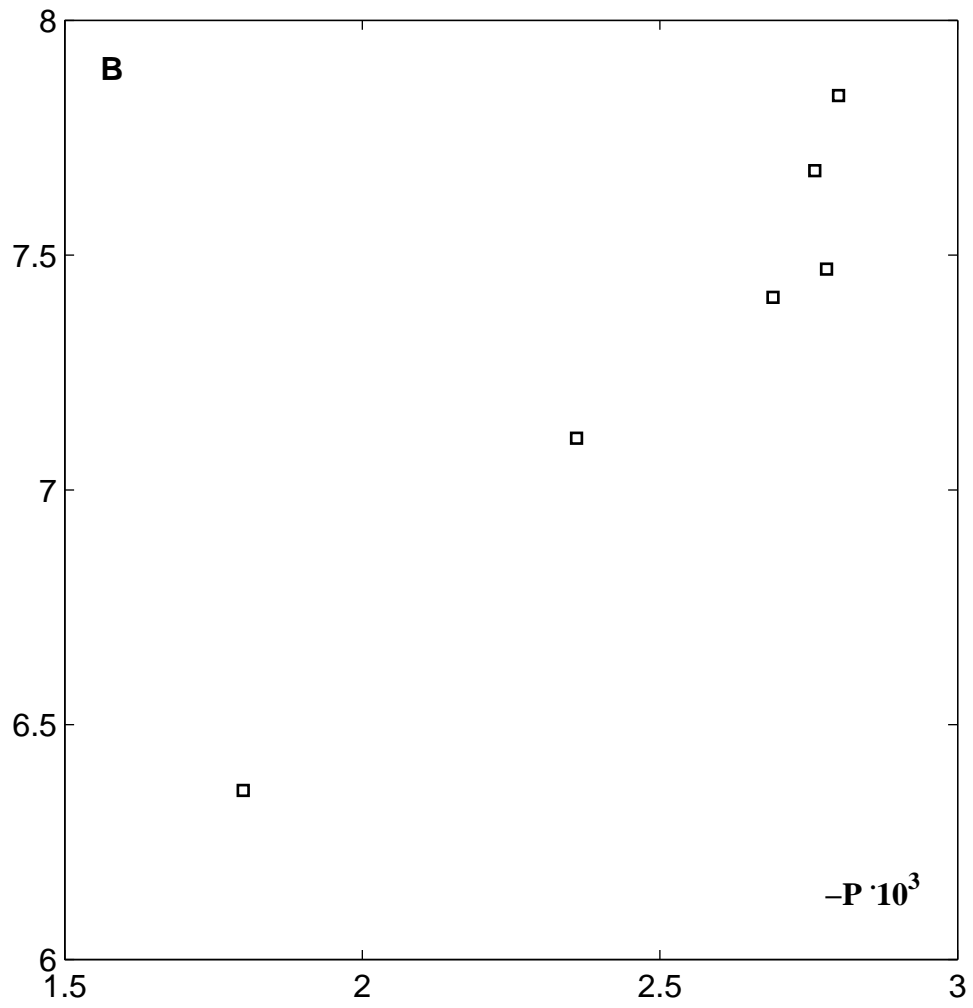


Figure 3 d

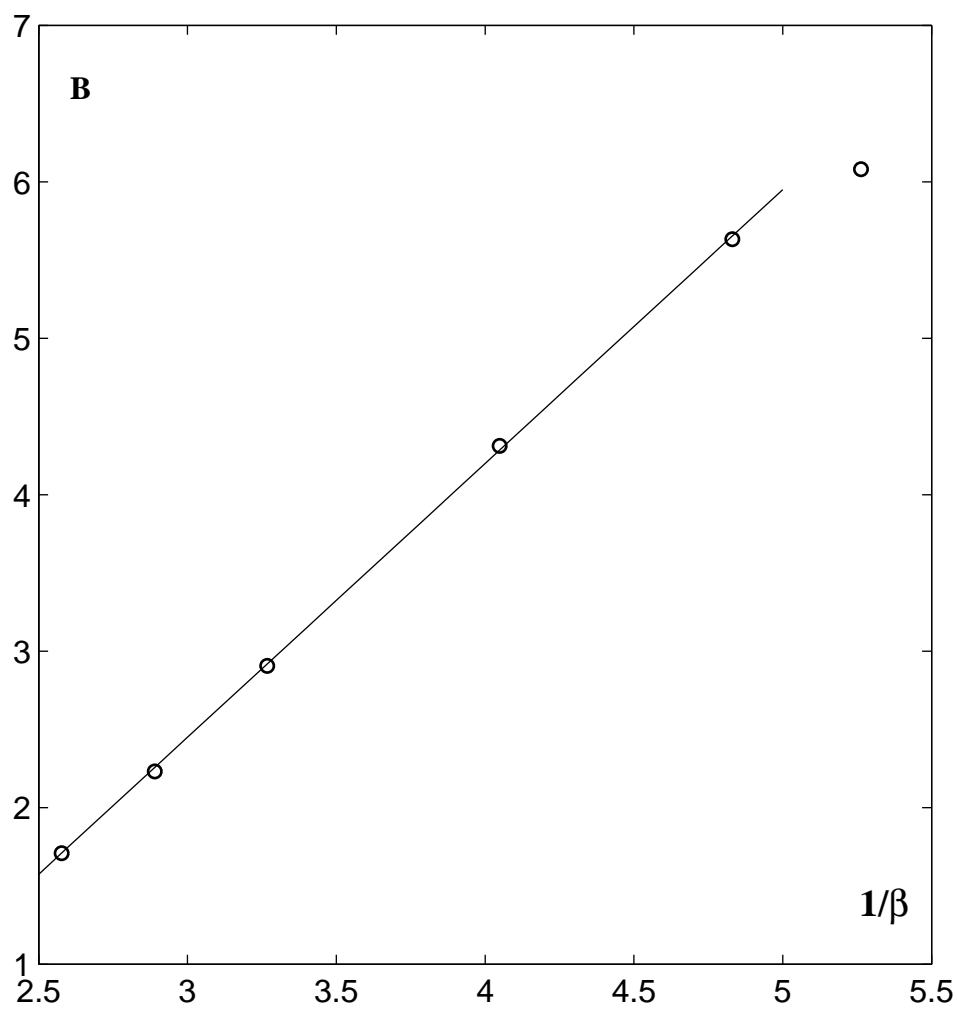


Figure 4 a

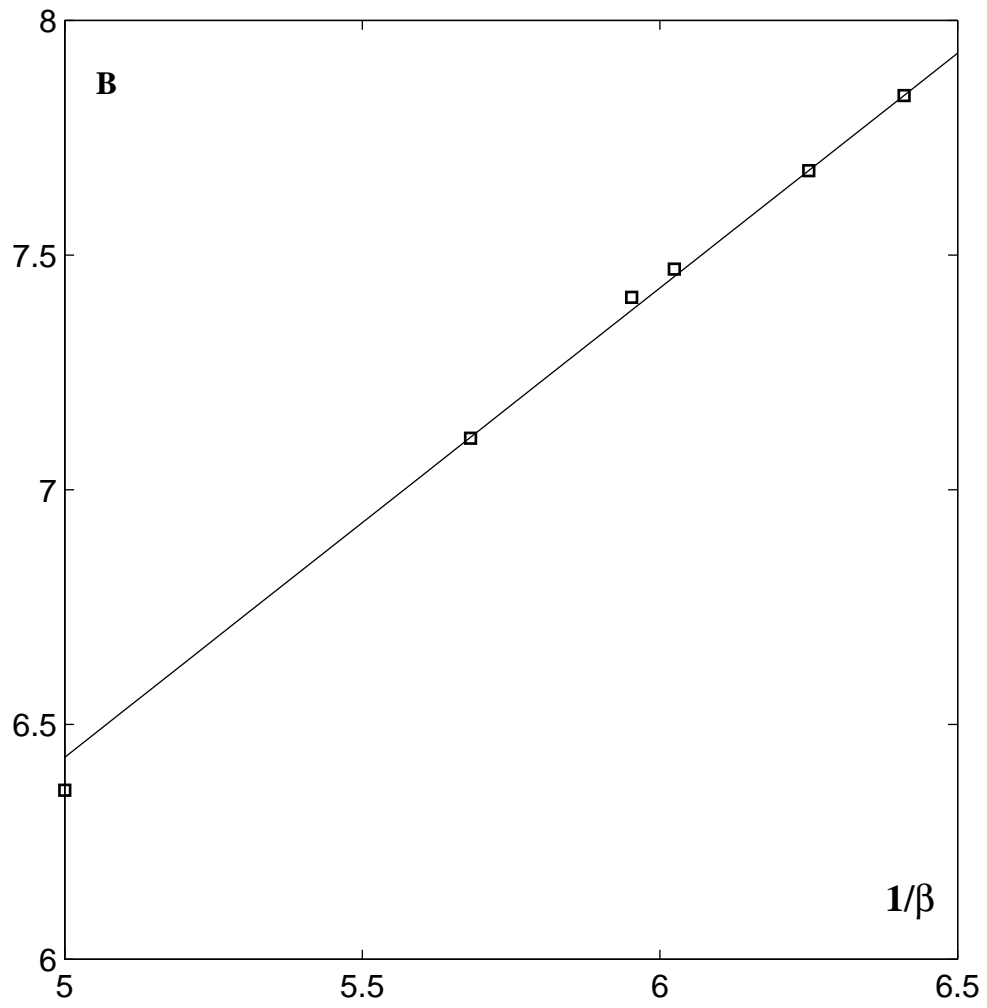


Figure 4 b